HHS Public Access

Author manuscript

Stroke. Author manuscript; available in PMC 2018 August 01.

Published in final edited form as:

Stroke. 2017 August ; 48(8): 2231–2237. doi:10.1161/STROKEAHA.117.017758.

Extracellular mitochondria in cerebrospinal fluid and neurological recovery after subarachnoid hemorrhage

Sherry Hsiang-Yi Chou, M.D.[1,2,3], **Jing Lan, M.D.**[1,4], **Elga Esposito, Ph.D.**[1], **MingMing Ning, M.D.**[1,5], **Leonora Balaj, Ph.D.**[6], **Xunming Ji, M.D., Ph.D.**[4], **Eng H. Lo, Ph.D.**[1,5], and **Kazuhide Hayakawa, Ph.D.**[1]

[1]Neuroprotection Research Laboratories, Departments of Radiology and Neurology, Massachusetts General Hospital and Harvard Medical School, Boston, MA, USA

[2]Departments of Critical Care Medicine, Neurology and Neurosurgery, University of Pittsburgh, Pittsburgh, PA, USA

[3]Department of Neurology, Brigham and Women's Hospital and Harvard Medical School, Boston, MA, USA

[4]Cerebrovascular Research Center, Xuanwu Hospital, Capital Medical University, Beijing, China

[5]Clinical Proteomics Research Center, Department of Neurology, Massachusetts General Hospital and Harvard Medical School, Boston, MA, USA

[6]Department of Neurology, Massachusetts General Hospital and Program in Neuroscience, Harvard Medical School, Boston, MA, USA

Abstract

Background and Purpose—Recent studies suggest that extracellular mitochondria may be involved in the pathophysiology of stroke. In this study, we assessed the functional relevance of endogenous extracellular mitochondria in cerebrospinal fluid (CSF) in rats and humans after subarachnoid hemorrhage (SAH).

Methods—A standard rat model of SAH was used, where an intraluminal suture was used to perforate a cerebral artery, thus leading to blood extravasation into subarachnoid space. At 24 and 72 hrs post-SAH, neurological outcomes were measured, and the standard JC1 assay was used to quantify mitochondrial membrane potentials in the CSF. To further support the rat model experiments, CSF samples were obtained from 41 SAH patients and 27 control subjects. Mitochondrial membrane potentials were measured with the JC1 assay, and correlations with clinical outcomes were assessed at 3 months.

Results—In the standard rat model of SAH, extracellular mitochondria was detected in CSF at 24 and 72 hrs after injury. JC1 assays demonstrated that mitochondrial membrane potentials in

Corresponding author: Kazuhide Hayakawa or Eng H. Lo, khayakawa1@partners.org or Lo@helix.mgh.harvard.edu, Neuroprotection Res Lab, MGH 149-2401, 13th Street, Charlestown, MA 02129, USA, Tel: 617-726-4043, Fax: 617-726-7830.

Competing Interests: The authors declare they have no competing financial interest.

Disclosures: "MITOCHONDRIAL BIOMARKERS OF, AND THERAPEUTICS FOR, CNS INJURY AND DISEASE" was filed in the United States Patent and Trademark Office as Application 62/381,917. Inventors: Sherry Hsiang-Yi Chou, MingMing Ning, Eng H. Lo, Kazuhide Hayakawa

CSF were decreased after SAH compared with sham-operated controls. In human CSF samples, extracellular mitochondria were also detected, and JC1 levels were also reduced after SAH. Furthermore, higher mitochondrial membrane potentials in the CSF was correlated with good clinical recovery at 3 months after SAH onset.

Conclusions—This proof-of-concept study suggests that extracellular mitochondria may provide a “biomarker-like” glimpse into brain integrity and recovery after injury.

Keywords

extracellular mitochondria; mitochondrial membrane potential; cerebrospinal fluid; subarachnoid hemorrhage

Introduction

Mitochondria comprise the intracellular energy source of cells. Because the brain is a high-metabolism organ, mitochondria play a central role in cerebral physiology and pathophysiology. During injury or disease, mitochondria may be a key regulator for neurodegeneration as well as neurorecovery, depending on its functionality [1–3].

Recently, emerging data in cell and animal models suggest that mitochondria can be released into extracellular space, and transferred from cell to cell [4–8]. In the central nervous system (CNS), retinal neurons may transfer mitochondria to astrocytes for disposal and recycling [9], and brain astrocytes may release extracellular mitochondria that could potentially support neuroplasticity after focal cerebral ischemia in mice [10]. However, it remains to be determined whether extracellular mitochondria may influence neurological outcomes in vivo.

In this study, we used a combination of experimental rat models and human samples from subarachnoid hemorrhage (SAH) patients to ask 3 questions. First, can functional extracellular mitochondria be detected in cerebrospinal fluid (CSF)? Second, are these extracellular mitochondria somehow perturbed after injury or disease? Third, if these signals are indeed altered after disease, is it possible that extracellular mitochondria may reflect the intracellular metabolic integrity of adjacent brain, thus providing a novel class of potential biomarkers for brain injury and recovery?

Methods

Rat Model of SAH

All experiments were performed following approved institutional protocols in accordance with the National Institute of Health Guide for the Care and Use of Laboratory Animals. Adult male Sprague–Dawley rats (320–350g, Charles River Laboratories) were used under isoflurane anesthesia (1.5% in 30%/70% oxygen/nitrous gas mix). Following standard procedures, SAH was performed by introducing a 3-0 prolene monofilament suture from the external carotid artery into the internal carotid artery and advancing it until resistance was experienced at the bifurcation of the internal carotid artery into the anterior and middle cerebral arteries. At this time, the suture was further advanced 5 mm to puncture the artery

and then it was quickly withdrawn. Sham-operated controls received the same procedure without inserting the filament. Animals were recovered for 24 hours, then all rats were assessed with the standard 5-point neuroscore scale to evaluate neurological outcomes [11]. CSF (at least 50 μL per rat) was collected from the cisterna magna for JC1 analysis. Six rats were used for sham-operated group, and 24 rats were subjected to SAH. Overall, 64% (9 out of 14) or 40% (4 out of 10) of rats survived at 24 hours or at 72 hours after SAH surgery, respectively. The relatively high mortality rates reflect the severity of this rat model, and these models did not receive rigorous medical care in an intensive care unit, unlike the human SAH patients (see below).

SAH subject recruitment and sample collection

Consecutive patients within 96 hours of onset of spontaneous, non-traumatic SAH were prospectively enrolled into a large SAH biomarker cohort study and serial blood and available CSF were collected and stored. CSF samples were collected only if patient has an external ventricular drain (EVD) placed for clinical indications. Patients with traumatic SAH, pregnancy, end-stage renal or hepatic disease, intracranial malignancies or infectious meningitis were excluded. Control subjects were patients undergoing trial of CSF diversion for evaluation of possible normal pressure hydrocephalus. All subjects were enrolled after informed consent and in accordance with institutional review board approved protocols. In both subject populations, serial CSF, serum, and plasma samples were immediately processed after collection. Samples were centrifuged at room temperature at 3900 RPM for 15 minutes and supinate was aliquotted and immediately frozen on dry ice and stored at −80°C until analysis.

Clinical variables and outcome assessment

Angiographic vasospasm was defined as >50% reduction in diameter of any intracerebral vessel on digital subtraction cerebral angiography (DSCA) on post-SAH day 6–8 compared with baseline. Per institutional clinical protocol, all SAH patients underwent DSCA) upon initial presentation and then again on post-SAH day 6–8 for evaluation of angiographic vasospasm. When multiple vessels were involved, vasospasm status was classified based on the most severely affected vessel. Long-term functional outcome were prospectively assessed at 3-month intervals using modified Rankin score (mRS) via standardized telephone interview. A standardized script was used to perform mRS scoring to reduce inter-rater variability. Poor outcome was defined as mRS>2.

Electron microscopy analysis

Following a centrifugation at 14,000 rpm for 20 minutes, pellets obtained from CSF samples were fixed in 2.0% glutaraldehyde in 0.1 M sodium cacodylate buffer, pH 7.4 (Electron Microscopy Sciences) for one hour at room temperature on a rocker. They were rinsed in cacodylate buffer, gently scraped and pelleted and post-fixed in 1.0% osmium tetroxide in cacodylate buffer for one hour on ice. They were rinsed in buffer and stabilized with a small amount of 2% agarose in PBS to hold them together. They were then dehydrated through a graded series of ethanol to 100%, followed by propylene oxide, 100%. They were infiltrated with Epon resin (Ted Pella) in a 1:1 solution of Epon:propylene oxide overnight on a rocker at room temperature. The following day they were placed in fresh Epon for several hours

and then embedded in Epon overnight at 60 °C. Thin sections were cut on a Leica EM UC7 ultramicrotome, collected on formvar-coated grids, stained with uranyl acetate and lead citrate and examined in a JEOL JEM 1011 transmission electron microscope at 80 kV. Images were collected using an AMT digital imaging system (Advanced Microscopy Techniques).

Western blot analysis

Western blot was performed as previously reported [12]. Each sample was loaded onto 4–20% Tris-glycine gels. After electrophoresis and transferring to nitrocellulose membranes, the membranes were blocked in Tris-buffered saline containing 0.1% Tween 20 and 0.2% I-block (Tropix) for 90 min at room temperature. Membranes were then incubated overnight at 4°C with following primary antibodies, anti-TOM40 (1:200, Santacruz) and anti-ANT1 antibody (1:200, Abcam). After incubation with peroxidase-conjugated secondary antibodies, visualization was enhanced by chemiluminescence (GE Healthcare).

FACS analysis

Standard FACS analysis was performed by BD Fortessa as described before [10]. To label mitochondria, MitoTracker Deep Red (100 nM, Thermo Fisher Scientific) or MitoTracker Red CMXRos (100 nM, Thermo Fisher Scientific) was used. Each fluorescent conjugated antibody such as vWF-FITC (1:500, Abcam), GLAST-APC (1:500, Miltenyl Biotec), CD45-FITC (1:500, Miltenyl Biotec), or CD41/CD61-FITC (1:500, Miltenyl Biotec) was added in CSF sample (100 μL) for 1 hour at room temperature. FACS analysis was performed using an unstained or phenotype control for determining appropriate gates, voltages, and compensations required in multivariate flow cytometry.

Mitochondria membrane potential measurement

Each rat CSF sample (100 μL; rat CSF 25 μL was diluted with 75μL PBS) or human CSF sample (100 μL) was incubated with JC1 (2 μL of 50 μM in 50% DMSO) for 20 min at 37 °C in 96-well MIcrofluor 1 plate (Thermo Fisher Scientific). JC1 dye exhibits potential-dependent accumulation in mitochondria, indicated by fluorescence emission shift from green (Ex 485 nm/Em 516 nm) to red (Ex 570 nm/Em 590 nm). Back ground fluorescent signal from each sample (100 μL containing 2 μL of 50% DMSO) was subtracted from JC1 fluorescent value and mitochondria membrane potential was determined by the red/green fluorescent ratio after top-read measurement in SpectraMax M5 microplate reader.

Statistical Methods

All of experiments were performed with full blinding, allocation concealment and randomization. Continuous variables were compared using student’s t or Wilcoxon Rank Sum test depending on data distribution normality. Depending on data normality, Pearson or Spearman correlation was used to measure strength of association between continuous variables. Multiple comparisons were evaluated by one-way ANOVA followed by Kruskal-Wallis test. All statistical analyses were performed using JMP Pro 12.1.0.

Results

JC1 mitochondrial membrane potential in rat CSF after SAH

To assess extracellular mitochondria in vivo, we collected rat CSF at 24 and 72 hours after SAH. Extracellular mitochondria were assessed with the standard JC1 assay (Supplemental figure I). JC1 green fluorescence (presumably reflecting mitochondria with collapsed membrane potentials) was significantly increased at 24 and 72 hours after SAH, and JC1 red fluorescence (presumably reflecting mitochondria with intact membrane potentials) was increased at 72 hours after SAH (Fig. 1A). Because total fluorescence signals may be correlated with mitochondrial density, these findings indirectly suggest that mitochondrial particle numbers in CSF may be elevated in these rat models of SAH. Next, we calculated the ratio of red-to-green JC1 signal, which is generally thought to reflect mitochondrial "integrity", i.e. the overall status of mitochondria with preserved membrane potentials. Compared with the sham-operated group, these JC1 ratio levels were lower at 24 hours after SAH, then JC1 ratios were slightly recovered at 72 hours, indicating the functional shift of mitochondria in the CSF (Fig. 1A). As expected, neuroscore measurements were elevated at 24 hours after SAH, consistent with neurological deficits (Fig. 1B). A regression analysis suggested that SAH-induced neurological deficits were inversely correlated with JC1 red-to-green ratios in the CSF (Fig. 1C).

Extracellular mitochondria in human CSF after SAH

CSF samples were obtained from 41 subarachnoid hemorrhage (SAH) patients and 27 normal control human subjects from a prospective SAH biomarker cohort study. Table 1 summarizes the clinical characteristics of both populations. Electron microscopy and western blot analysis confirmed the presence of extracellular mitochondria (Fig. 2A) and mitochondrial proteins (Fig. 2B) in CSF samples. We performed flow cytometry for all mitochondrial particles labeled with MitoTracker Deep Red FM, and the analysis revealed an increase in CSF extracellular mitochondrial particles after SAH (Fig. 2C).

Mitochondrial membrane potential in CSF and outcomes after SAH

Next we asked whether mitochondrial membrane potential could be detected in these CSF samples. Interestingly, mitochondrial membrane potential was significantly lower in SAH subjects compared with controls (Fig. 3A). There were no differences in size distribution and the percentage of mitochondria amongst all particles between good versus poor outcomes after SAH (Fig. 3B). However, there appeared to be an inverse relationship between membrane potential (JC1 red-to-green ratio) and brain injury severity. Subjects with higher SAH severity had lower CSF JC1 ratio levels on day 1 (Fig. 3C). Furthermore, recovery of JC1 ratio levels on day 3 was significantly associated with good outcomes at 3 months after SAH (Fig. 3D).

One potential confound is that CSF mitochondrial measurements in SAH may be contaminated by blood. If so, one would expect that CSF after SAH would have higher JC1 ratios than controls. The opposite was true here, with lower JC1 ratio levels in SAH cases. When mitochondrial membrane potentials were measured in plasma samples from the same patients, mitochondrial membrane potential was significantly lower in SAH subjects

compared with controls (Fig. 4A), and there was no correlation between blood JC1 levels and functional outcome (Fig. 4B), again suggesting that these responses in CSF may not be driven by blood contamination after SAH.

Finally, we explored the potential cellular origin of these CSF mitochondria signals found in SAH. Because extracellular mitochondria tend to be contained within membranous particles, cell-specific markers embedded in these membranes may provide indirect information on potential cellular origins. We performed flow cytometry for all functional mitochondria particles labeled with MitoTracker Red CMXRos, and assessed positive events for vWF (endothelial cell origin), GLAST (astrocyte), CD45 (microglia/macrophage), and CD41/CD61 (platelet) (Fig. 5A). Subjects with good outcomes at 3 month had a significantly higher percentage of GLAST-positive mitochondria particles in their CSF at day 3 post-SAH (Fig. 5B) but there was no correlation with other cellular origin markers (Fig. 5C), suggesting that responses in CSF extracellular mitochondria may be partly associated with astrocytic origins.

Discussion

Taken together, we found that (i) extracellular mitochondrial membrane potentials were reduced in rat CSF after SAH, (ii) reductions in mitochondria membrane potentials were also detectable in human CSF after SAH, (iii) higher mitochondrial membrane potentials in CSF were associated with good 3-month outcomes after SAH, and (iv) a higher proportion of mitochondria that were associated with good 3 month outcomes may be potentially linked to astrocytic origins.

In both rat models as well as human patients, extracellular mitochondrial function was detectable in normal CSF, and JC1 ratios were decreased after SAH. Therefore, assessment of mitochondrial function in CSF may provide an indirect way to assess brain injury; lower CSF mitochondrial membrane potentials indicate damaged brain whereas higher CSF membrane potentials may indicate metabolic recovery. But there are several important caveats. First, it is unclear whether CSF mitochondria particles represent some type of active release or merely reflect passive release or even debris from compromised cells. The fact that mitochondrial membrane potential was measurable and higher in control CSF than in SAH, and higher CSF membrane potentials were associated with better SAH outcomes, might argue against the worry that CSF mitochondrial particles simply represent uninformative debris. Further studies are required to investigate mitochondrial trafficking mechanisms in injured human brain. Second, JC1 values may be affected by the dye concentrations used. It is known that a high concentration of JC1 may produce non-specific dye aggregation giving a potentially imperfect indication of mitochondrial membrane potential. Prior to these studies, we tried to optimize JC1 dye concentrations for our model systems (Supplemental figure I), but future experiments testing other mitochondria dyes (e.g. TMRE) may be useful. Third, it should be noted that our initial human data are relatively limited and control subjects, while they have no acute brain injury, may not be “completely healthy” since they comprise patients suspected of having normal pressure hydrocephalus. Fourth, we do not know why CSF mitochondrial membrane potentials in the early stages of SAH can predict later outcomes. Nevertheless, our findings may be consistent

with the recent idea of early brain injury as the key pathologic mechanism in SAH [13]. This phenomenon begins immediately after cerebral hemorrhage, and is known to trigger cell death along with mitochondrial dysfunction [14]. Our CSF mitochondrial membrane potential measurements at day 1 after SAH showed significant reduction compared to controls, and recovery in these values at day 3 appear to correspond with patient outcomes. Hence, extracellular mitochondria in CSF may be a candidate biomarker that connects early brain injury mechanisms with recovery after SAH. Whether and how extracellular mitochondria may mechanistically connect to delayed vascular sequelae of SAH (vasospasm, perturbations in hemostasis and fibrinolysis, cerebral ischemia etc) [15, 16] remain to be determined. Fifth, mitochondria are highly dynamic entities with highly responsive profiles of fission and fusion [3]. How mitochondrial dynamics may affect our extracellular hypothesis requires further consideration. A sixth caveat relates to blood contamination in CSF. The lack of correlation between blood mitochondrial levels and CSF levels suggest that this might not be a major concern. However, a fraction of all CSF mitochondria were still positive for platelet markers suggesting blood origins [17]. If so, then patients with more subarachnoid blood may have a larger component coming from blood, and this may dilute the connection between CSF signals with brain metabolism per se. A seventh caveat relates to cellular origins. We performed FACS analysis to identify the potential cellular origin of extracellular mitochondria by MitoTracker CMXRos and each cell surface marker. But, this method only works for mitochondria contained within membranous particles. The cellular origins of “naked” mitochondria may be more difficult to ascertain. Eighth, all human samples underwent freeze-thaw. Although we found that JC1 values after freeze-thaw cycling were close to initial JC1 values (Supplemental figure I), better methods to preserve mitochondrial quality should be explored. Ninth, CSF mitochondrial measurements in SAH patients may be influenced by age (Supplemental figure II). Optimizing age-appropriate thresholds may eventually be necessary to better assess clinical outcomes in wider cohorts of patients. Additionally, other factors such as gender [18–21] and genetic background [22] may also influence SAH outcome. Future studies should further validate CSF JC1 endpoints in larger and separate patient cohorts. Tenth, our data implicate that JC1 may be useful to assess brain integrity. But other exosomes presenting in CSF may be also important to confer disease pathology [23–25]. How specifically CSF mitochondrial function reflects brain pathological state remain to be fully addressed. Finally, we acknowledge that our observations only indicate a general relationship between extracellular mitochondria and underlying brain tissue integrity. Deeper studies are required to connect these CSF signals with multifactorial mechanisms of hemorrhagic brain injury [26–30], and perhaps fit these ideas into the broader concept of help-me signaling within the remodeling neurovascular unit [31].

Summary/Conclusions

Taken together, these data demonstrate that extracellular mitochondria are altered in the CSF after SAH. Perhaps most importantly, this proof-of-concept study suggests that this may not just be an “experimental phenomenon”; extracellular mitochondria are indeed detectable in humans, and these measurements may be functionally correlated with patient outcomes after SAH. Existing efforts to find biomarkers for brain damage typically involve intracellular and membrane proteins [32, 33]. This study suggests that extracellular mitochondria may represent

a potentially new class of signals worth pursuing. The JC1 assay is relatively fast and easy to use, so these measurements may be potentially applicable at the patient bedside. Further studies are warranted to investigate this idea and assess its applicability for a wider range of CNS disorders.

Supplementary Material

Refer to Web version on PubMed Central for supplementary material.

Acknowledgments

Electron microscopy was performed in the Center for Systems Biology, Massachusetts General Hospital. Cytometric assessments were supported by the MGH Department of Pathology Flow and Image Cytometry Core. Thanks to Dr. Xandra O. Breakefield for helpful discussion.

Sources of Funding

This work was supported in part by grants from NIH, the Rappaport Foundation, and the China National Natural Science Foundation Award For Distinguished Young Scholars.

References

1. Lin MT, Beal MF. Mitochondrial dysfunction and oxidative stress in neurodegenerative diseases. Nature. 2006; 443:787–795. [PubMed: 17051205]
2. Anne Stetler R, Leak RK, Gao Y, Chen J. The dynamics of the mitochondrial organelle as a potential therapeutic target. J Cereb Blood Flow Metab. 2013; 33:22–32. [PubMed: 23093069]
3. Balog J, Mehta SL, Vemuganti R. Mitochondrial fission and fusion in secondary brain damage after cns insults. J Cereb Blood Flow Metab. 2016; 36:2022–2033. [PubMed: 27677674]
4. Islam MN, Das SR, Emin MT, Wei M, Sun L, Westphalen K, et al. Mitochondrial transfer from bone-marrow-derived stromal cells to pulmonary alveoli protects against acute lung injury. Nat Med. 2012; 18:759–765. [PubMed: 22504485]
5. Ahmad T, Mukherjee S, Pattnaik B, Kumar M, Singh S, Rehman R, et al. Miro1 regulates intercellular mitochondrial transport & enhances mesenchymal stem cell rescue efficacy. EMBO J. 2014; 33:994–1010. [PubMed: 24431222]
6. Tan AS, Baty JW, Dong LF, Bezawork-Geleta A, Endaya B, Goodwin J, et al. Mitochondrial genome acquisition restores respiratory function and tumorigenic potential of cancer cells without mitochondrial DNA. Cell Metab. 2015; 21:81–94. [PubMed: 25565207]
7. Dong LF, Kovarova J, Bajzikova M, Bezawork-Geleta A, Svec D, Endaya B, et al. Horizontal transfer of whole mitochondria restores tumorigenic potential in mitochondrial DNA-deficient cancer cells. Elife. 2017:6.
8. Masuzawa A, Black KM, Pacak CA, Ericsson M, Barnett RJ, Drumm C, et al. Transplantation of autologously derived mitochondria protects the heart from ischemia-reperfusion injury. Am J Physiol Heart Circ Physiol. 2013; 304:H966–982. [PubMed: 23355340]
9. Davis CH, Kim KY, Bushong EA, Mills EA, Boassa D, Shih T, et al. Transcellular degradation of axonal mitochondria. Proc Natl Acad Sci U S A. 2014; 111:9633–9638. [PubMed: 24979790]
10. Hayakawa K, Esposito E, Wang X, Terasaki Y, Liu Y, Xing C, et al. Transfer of mitochondria from astrocytes to neurons after stroke. Nature. 2016; 535:551–555. [PubMed: 27466127]
11. Turan N, Miller BA, Heider RA, Nadeem M, Sayeed I, Stein DG, et al. Neurobehavioral testing in subarachnoid hemorrhage: A review of methods and current findings in rodents. J Cereb Blood Flow Metab. 2016 271678X16665623.
12. Hayakawa K, Pham LD, Katusic ZS, Arai K, Lo EH. Astrocytic high-mobility group box 1 promotes endothelial progenitor cell-mediated neurovascular remodeling during stroke recovery. Proc Natl Acad Sci U S A. 2012; 109:7505–7510. [PubMed: 22529378]

13. Chen S, Feng H, Sherchan P, Klebe D, Zhao G, Sun X, et al. Controversies and evolving new mechanisms in subarachnoid hemorrhage. Prog Neurobiol. 2014; 115:64–91. [PubMed: 24076160]
14. Chen S, Wu H, Tang J, Zhang J, Zhang JH. Neurovascular events after subarachnoid hemorrhage: Focusing on subcellular organelles. Acta Neurochir Suppl. 2015; 120:39–46. [PubMed: 25366597]
15. Jabbarli R, Reinhard M, Roelz R, Shah M, Niesen WD, Kaier K, et al. Early identification of individuals at high risk for cerebral infarction after aneurysmal subarachnoid hemorrhage: The behavior score. J Cereb Blood Flow Metab. 2015; 35:1587–1592. [PubMed: 25920954]
16. Boluijt J, Meijers JC, Rinkel GJ, Vergouwen MD. Hemostasis and fibrinolysis in delayed cerebral ischemia after aneurysmal subarachnoid hemorrhage: A systematic review. J Cereb Blood Flow Metab. 2015; 35:724–733. [PubMed: 25690473]
17. Boudreau LH, Duchez AC, Cloutier N, Soulet D, Martin N, Bollinger J, et al. Platelets release mitochondria serving as substrate for bactericidal group iia-secreted phospholipase a2 to promote inflammation. Blood. 2014; 124:2173–2183. [PubMed: 25082876]
18. Kongable GL, Lanzino G, Germanson TP, Truskowski LL, Alves WM, Torner JC, et al. Gender-related differences in aneurysmal subarachnoid hemorrhage. J Neurosurg. 1996; 84:43–48. [PubMed: 8613834]
19. Eden SV, Meurer WJ, Sanchez BN, Lisabeth LD, Smith MA, Brown DL, et al. Gender and ethnic differences in subarachnoid hemorrhage. Neurology. 2008; 71:731–735. [PubMed: 18550859]
20. Friedrich V, Bederson JB, Sehba FA. Gender influences the initial impact of subarachnoid hemorrhage: An experimental investigation. PLoS One. 2013; 8:e80101. [PubMed: 24250830]
21. Turan N, Heider RA, Zaharieva D, Ahmad FU, Barrow DL, Pradilla G. Sex differences in the formation of intracranial aneurysms and incidence and outcome of subarachnoid hemorrhage: Review of experimental and human studies. Transl Stroke Res. 2016; 7:12–19. [PubMed: 26573918]
22. D'Abbondanza JA, Ai J, Lass E, Wan H, Brathwaite S, Tso MK, et al. Robust effects of genetic background on responses to subarachnoid hemorrhage in mice. J Cereb Blood Flow Metab. 2016; 36:1942–1954. [PubMed: 26661216]
23. Stuendl A, Kunadt M, Kruse N, Bartels C, Moebius W, Danzer KM, et al. Induction of alpha-synuclein aggregate formation by csf exosomes from patients with parkinson's disease and dementia with lewy bodies. Brain. 2016; 139:481–494. [PubMed: 26647156]
24. Yagi Y, Ohkubo T, Kawaji H, Machida A, Miyata H, Goda S, et al. Next-generation sequencing-based small rna profiling of cerebrospinal fluid exosomes. Neurosci Lett. 2017; 636:48–57. [PubMed: 27780738]
25. Riancho J, Vazquez-Higuera JL, Pozueta A, Lage C, Kazimierczak M, Bravo M, et al. Microrna profile in patients with alzheimer's disease: Analysis of mir-9-5p and mir-598 in raw and exosome enriched cerebrospinal fluid samples. J Alzheimers Dis. 2017; 57:483–491. [PubMed: 28269782]
26. Suzuki H, Shiba M, Nakatsuka Y, Nakano F, Nishikawa H. Higher cerebrospinal fluid ph may contribute to the development of delayed cerebral ischemia after aneurysmal subarachnoid hemorrhage. Transl Stroke Res. 2017; 8:165–173. [PubMed: 27623837]
27. Aronowski J, Zhao X. Molecular pathophysiology of cerebral hemorrhage: Secondary brain injury. Stroke. 2011; 42:1781–1786. [PubMed: 21527759]
28. Suarez JI, Tarr RW, Selman WR. Aneurysmal subarachnoid hemorrhage. N Engl J Med. 2006; 354:387–396. [PubMed: 16436770]
29. Wang KC, Tang SC, Lee JE, Li YI, Huang YS, Yang WS, et al. Cerebrospinal fluid high mobility group box 1 is associated with neuronal death in subarachnoid hemorrhage. J Cereb Blood Flow Metab. 2017; 37:435–443. [PubMed: 26823474]
30. Winkler MK, Dengler N, Hecht N, Hartings JA, Kang EJ, Major S, et al. Oxygen availability and spreading depolarizations provide complementary prognostic information in neuromonitoring of aneurysmal subarachnoid hemorrhage patients. J Cereb Blood Flow Metab. 2017; 37:1841–1856. [PubMed: 27025768]
31. Xing C, Lo EH. Help-me signaling: Non-cell autonomous mechanisms of neuroprotection and neurorecovery. Prog Neurobiol. 2016
32. Yang Z, Wang KK. Glial fibrillary acidic protein: From intermediate filament assembly and gliosis to neurobiomarker. Trends Neurosci. 2015; 38:364–374. [PubMed: 25975510]

33. Kobeissy FH, Guingab-Cagmat JD, Zhang Z, Moghieb A, Glushakova OY, Mondello S, et al. Neuroproteomics and systems biology approach to identify temporal biomarker changes post experimental traumatic brain injury in rats. Front Neurol. 2016; 7:198. [PubMed: 27920753]

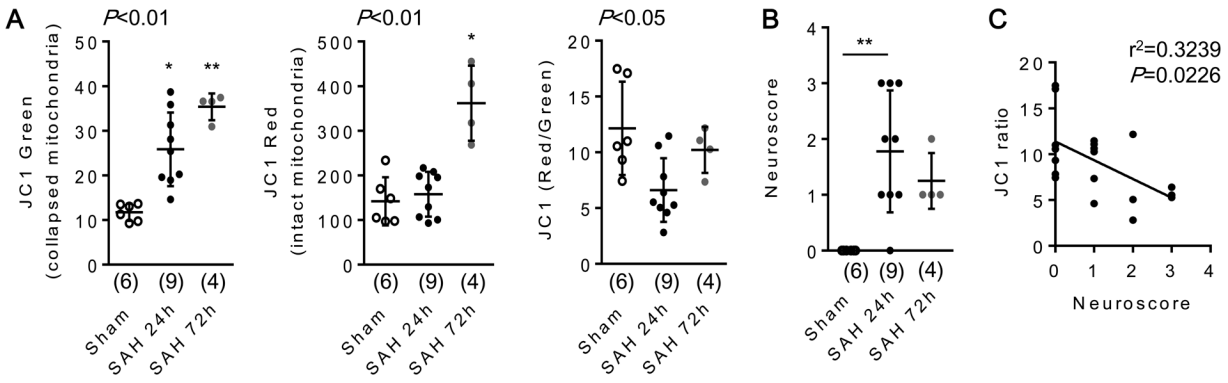

Figure 1. Extracellular mitochondrial functional assay in a rat subarachnoid hemorrhage (SAH) model in vivo

Rats were subjected to subarachnoid hemorrhage (SAH) by endovascular perforation, and CSF samples were collected at 24 and 72 hours after SAH onset. JC1 green or JC1 red indicates collapsed mitochondria or intact mitochondria, respectively. **A.** CSF JC1 value at 24 hours after SAH was lower than sham-operated group. Then, JC1 value was slightly recovered at 72 hours after SAH. Sham; n=6, SAH 24h; n=9, SAH 72h; n=4. **P*<0.05, ***P*<0.01 vs Sham. **B.** Neuroscore was significantly higher at 24 hours after SAH compared with sham-operated group. ***P*<0.01. **C.** Regression analysis demonstrated that JC1 ratio was inversely correlated with Neuroscore after SAH. Note: lower CSF volumes collected from the rat SAH models preclude the use of FACS to perform true particle quantification (see human data in Figure 2 below).

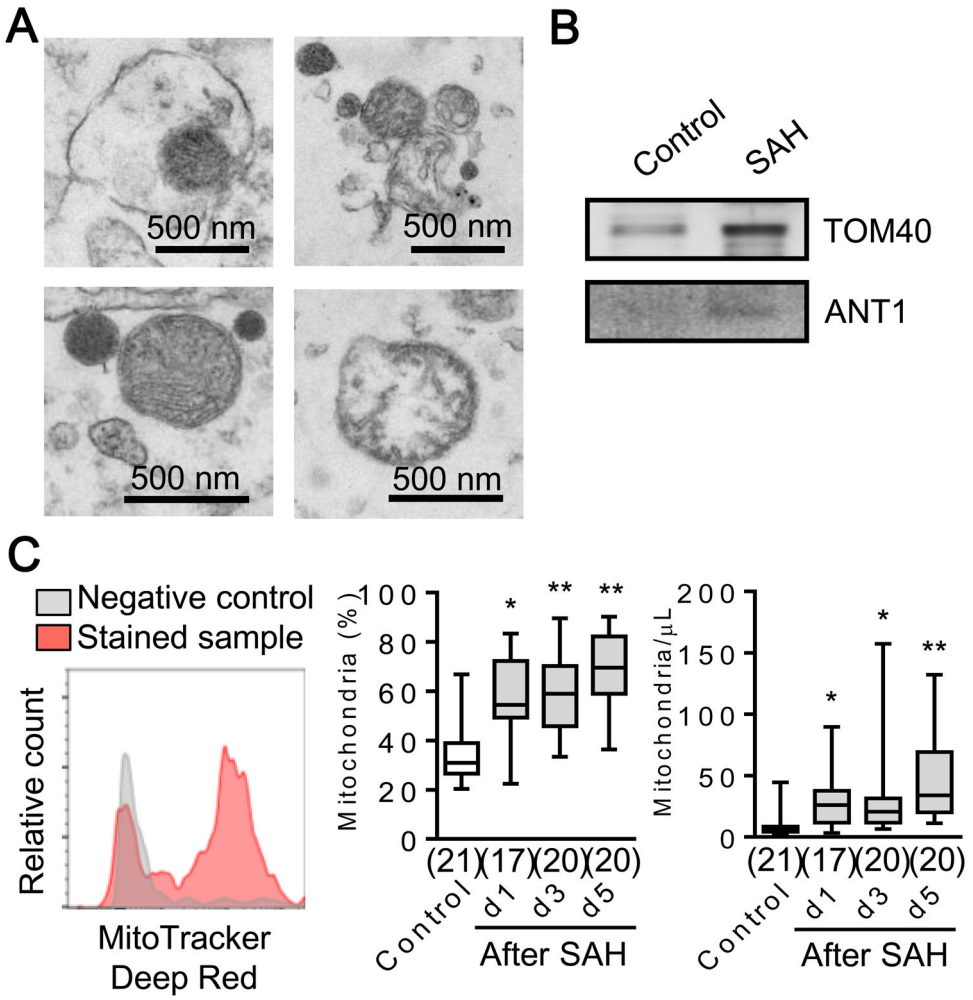

Figure 2. Assessment of extracellular mitochondria in human CSF after SAH

A. Transmission electron microscopy (TEM) of extracellular mitochondria in CSF collected from patients at 3 days after SAH. Scale: 500 nm. **B.** Western blot confirmed expressions of mitochondrial outer membrane protein (TOM40) and inner membrane protein (ANT1) in CSF. **c,** Each CSF sample (100 μL) was incubated with MitoTracker Deep Red (10 μL, 1 μM) for 20 min at 37°C. FACS analysis showed significant increase of extracellular mitochondria in CSF overtime after SAH. *P<0.05, **P<0.01 vs Control.

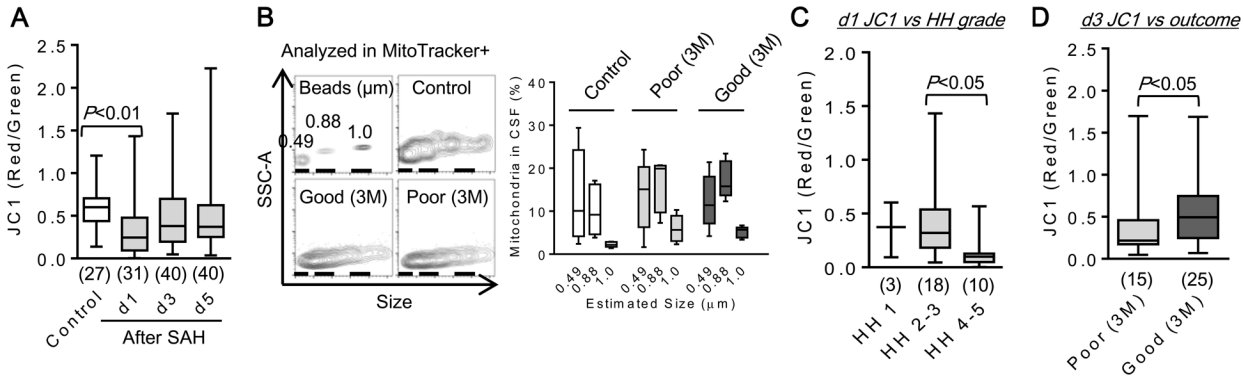

Figure 3. Extracellular mitochondrial function was associated with outcome after SAH

A. Each CSF sample (100 μl) was incubated with 50 μM JC1 (2 μL) for 20 min at 37°C. JC1 value at day 1 after SAH was significantly lower than control subjects. **B.** Mitochondrial size ranging from 490 nm to 1 μm and the frequency were measured with FACS analysis. There was no clear difference in size and percentage of CSF mitochondria among study subject groups (each n=5). **C.** A lower JC1 at day 1 after SAH was associated with a higher Hunt & Hess (HH) grade. **D.** JC1 value was higher in good clinical outcome compared to poor outcome at 3 month after SAH.

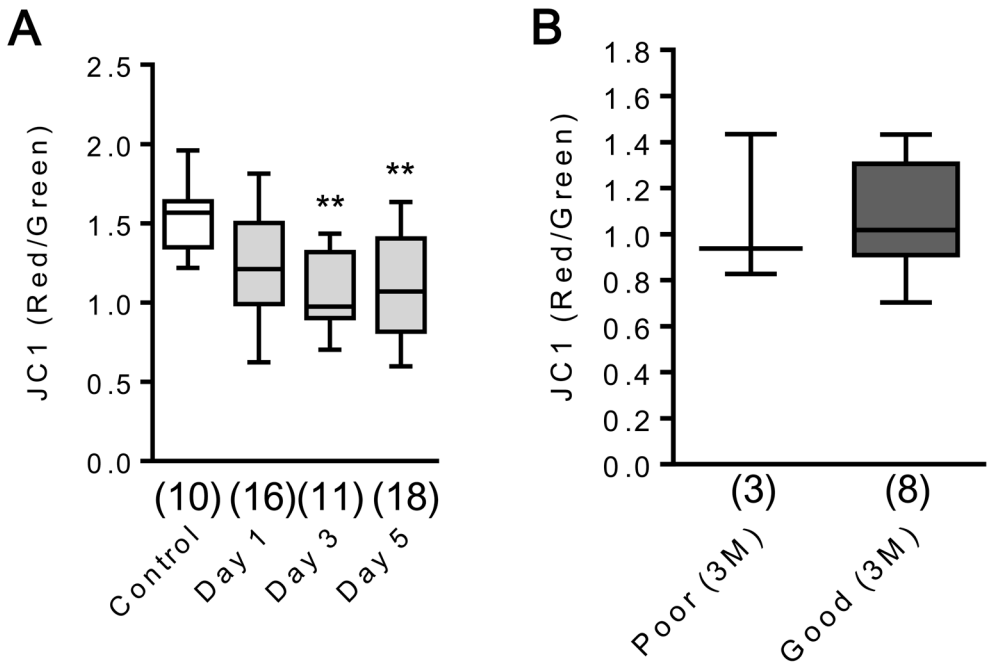

Figure 4. JC1 analysis in plasma samples

A. Plasma mitochondrial membrane potential was significantly decreased at days 3 and 5 after SAH. ** $P<0.01$ vs Control. **B.** There was no significant difference in plasma JC1 value between good and poor outcome at 3 months post SAH.

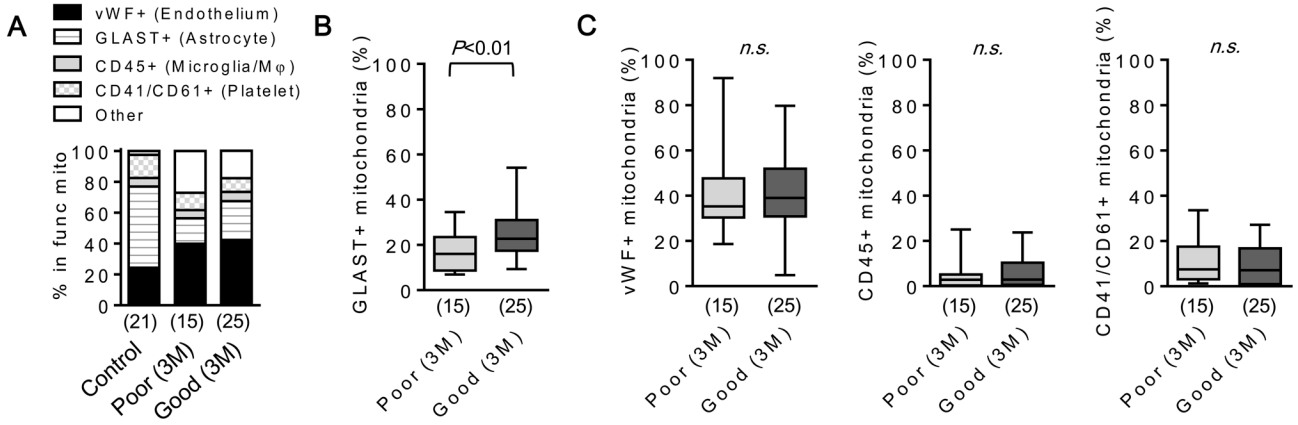

Figure 5. An increase of astrocyte-originated mitochondria may be correlated with good outcome after SAH

A. Functional mitochondria in CSF was labeled by MitoTracker Red CMXRox (100 nM). Each cell type marker such as vWF-FITC (endothelial cell), GLAST-APC (astrocyte), CD45-FITC (microglia/macrophage), or CD41/CD61-FITC (platelet) was co-incubated with CSF. Of MitoTracker positive events in FACS, positive population for each cell type marker was identified. **B.** FACS analysis showed that SAH subjects with good outcome at 3 month has higher percentage of GLAST+ mitochondria in CSF. **C.** There were no difference in percentage of vWF+, CD45+, and CD41/CD61+ events between good and poor outcome groups.

Table 1

	SAH (N = 41)	Control (N = 27)
Age (mean)	51.8(47.1 – 56.4)	73.1 (68.9–77.2)
Sex		
Women	25 (61%)	3 (11%)
Men	16 (39%)	24 (89%)
Hunt and Hess Grade		n/a
1	4 (10%)	
2	12 (29%)	
3	11 (27%)	
4	9 (22%)	
5	5 (12%)	
Modified Fisher Grade		n/a
1		
2	0	
3	5 (12%)	
4	34 (83%)	
	2 (5%)	
Aneurysm Location		n/a
Pcomm	6 (15%)	
Acomm	21 (51%)	
Basilar	3 (7%)	
PICA	3 (7%)	
ICA	2 (5%)	
MCA	2 (5%)	
ACA	1 (2%)	
angionegative	3 (7%)	
Aneurysm Treatment		n/a
Craniotomy + Clip	19 (46%)	
Endovascular Coil	17 (41%)	
Other	5 (12%)	
Vasospasm		n/a
Yes	24 (59%)	
No	17 (41%)	
Delayed Cerebral Ischemia (DCI)		n/a
Yes	5 (12%)	
No	36 (88%)	
3 month mRS		n/a

	SAH (N = 41)	Control (N = 27)
<= 2 (Good)	25 (61%)	
> 2 (Poor)	16 (39%)	
6 month mRS		n/a
<= 2 (Good)	28 (70%)	
> 2 (Poor)	12 (30%)	